



22nd IAHR International Symposium on Ice
Singapore, August 11 to 15, 2014

**Propeller Blade Impact Forces Due to Cavitation Cloud Collapse by
Using a Coupled Eulerian-Lagrangian Method**

Ville S. Lämsä, Juha Virtanen, Aki Kinnunen and Pekka Koskinen

VTT Technical Research Center of Finland

P.O. Box 1000, FI-02044 VTT, Finland

{ville.s.lamsa, juha.virtanen, aki.kinnunen, pekka.koskinen}@vtt.fi

Cavitation is a significant cause of wear, noise and loss of efficiency in marine propellers. In this study the impact forces due to cavitation cloud collapse are investigated in context of ice-propeller interaction. Force measurements from the propeller blade indicate that the hydrodynamic non-contact forces are relevant when the loads on the blade are developed during the ice-propeller interaction. According the measurement one could claim that the measured short duration force peaks are due to cavitation cloud collapse. These cavitation clouds originate from the previous blade while milling the ice block and collapse once arriving on the pressure side of the next blade. In this article the coupled Eulerian-Lagrangian method is used to efficiently compute the impact forces generated by the collapse of the cavitation clouds. The results of the impact forces show that the peak impact forces due to collapse of the ice-induced cavitation clouds are high enough to damage the propeller blade. Thus the presented results do not prevent a possibility that the measured force peaks would be caused by the collapse of the cavitation clouds. The results of the impact forces can be thereafter also used to develop simplified formulas for the cavitation loading which, on the other hand, can be used for example on the basis of the ice rules.

1. Introduction

The formation of bubbles in a fluid is known as cavitation. In case of marine propellers a low-pressure voids, bubbles or bubble clouds are formed as water accelerates around and moves past the propeller blades. According to the Bernoulli's principle the faster the blades move, the lower the pressure around them become. As the pressure reaches the vapour pressure, water vaporizes and forms small bubbles of gas. Vapour gases evaporate into the cavity from the surrounding water. Therefore the cavity is not a perfect vacuum, but has a relatively low gas pressure. Such a low-pressure cavitation bubble begins to collapse due to the higher pressure of the surrounding water. The bubble eventually collapses by releasing a significant amount of energy, and this is followed by successive rebounds and collapses. The shock waves formed by collapse may be audible and strong enough to damage the propeller blades due to cyclic stress.

According to the ITTC (2002) there are five types of cavitation in marine propellers: root cavitation, hub and tip vortex cavitation, sheet cavitation, bubble cavitation and cloud cavitation. In this study the impact forces due to cavitation cloud collapse are investigated in context of ice-propeller interaction. Namely, several force measurements (e.g. Duff et al. (1985), Laskow & Revill (1986), Lindroos & Björkestam (1986), Jussila & Koskinen (1989a, 1989b), Keinonen & Browne (1990) and Brown et al. (1991a, 1991b)) from the propeller blade indicate that the hydrodynamic non-contact forces are relevant when the loads on the blade are developed during the ice-propeller interaction. It is claimed that the measured short duration equidistant force peaks are due to cavitation cloud collapse. These cavitation clouds originate from the previous blade while milling to the ice block and collapse once arriving on the pressure side of the next blade. Generation of the ice-induced cavitation clouds and their collapse is illustrated in Figures 1 and 2.

Traditionally cavitation phenomenon has been studied by using the computational fluid dynamics (CFD). This method has been successfully applied to the vast number of applications such as propeller-fluid and ship hull-fluid interactions. However, when impact forces, generated from a collapse of the low-pressure cavitation cloud, are in focus, other methods can offer significant computational benefits.

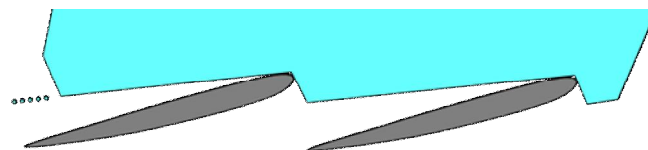


Figure 1. The leading edge of the propeller blade comes into contact with ice. The interaction occurs usually in milling-type conditions.

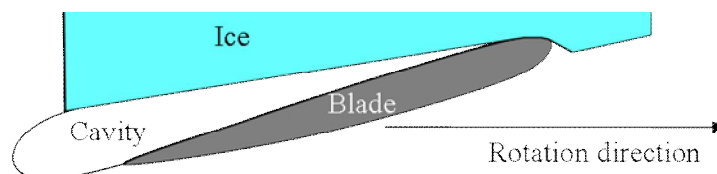


Figure 2. Generation of the ice-induced cavitation clouds. The cloud is originating from the suction side of the propeller blade during the ice-propeller interaction.

In this article the CEL method is used to efficiently compute the impact forces generated by the collapse of the cavitation cloud which are acting on a propeller blade. The results of the impact forces can be thereafter used to develop simplified formulas for the cavitation loading which, on the other hand, can be used for example on the basis of the ice rules. The main advantage of the CEL method is that the computational burden is relieved substantially compared to the CFD methods. Therefore the relative positions and sizes of the cavitation clouds and the propeller blade geometry can be changed easily allowing the further investigation of the impact forces.

2. Methods and Analyses

Using a coupled Eulerian-Lagrangian (CEL) method, cloud cavitation impact forces can be studied as a fluid-cavity interaction through a contact. The pure Eulerian analysis allows for effective modelling of extreme deformation such as fluid flow. When the Eulerian analysis is coupled with the traditional Lagrangian analysis, interactions between highly deformable material and rigid or relatively stiff bodies such as in fluid-structure interactions can be modelled.

Analyses are done by using Abaqus 6.12-3 program. Since the CEL therein is just a straightforward implementation of the full CFD method without a separate cavitation model, the initial cavity needs to be given for it. Therefore the starting point of the analyses is the moment when the ice-induced artificially created cavity is in its largest. For the sake of simplicity, the initial cavity is assumed to be completely void and sphere. Four different sizes of the cavity are used – cavitation cloud radii of 0.1, 0.2, 0.4 and 0.8 meters, and three different (smallest) distances of the cavitation cloud to the blade: 0.0 (in point contact), 0.1 and 0.2 meters.

The assembly for the analyses is shown in Figure 3. The generic Lagrangian Ni-Br-Al ($\rho = 7580 \text{ kg/m}^3$, $E = 123 \text{ GPa}$) propeller blade is placed to the 7 meter deep circular water cylinder. The depth at the tip of the blade is 4 meters. The diameter of the propeller is 3.9 meters and the diameter of the water cylinder is 5 meters. Water is modelled with the Mie-Grüneisen equation of state relation as Eulerian material ($\rho = 1000 \text{ kg/m}^3$, $\nu = 1.05 \times 10^{-3} \text{ kg/ms}$). A hard contact pressure-overclosure relationship without physical softening is used between the propeller blade and the water. The friction coefficient is assumed to be 0.2. A tensile failure model where the deviatoric stresses will be set to zero and pressure stress will be limited by the hydrostatic cutoff stress (0 Pa) is used.

Zero pressure boundary condition is used for the free surface of the water, and non-reflecting boundary conditions for the other surfaces of the circular water cylinder. Loads acting on the system are the hydrodynamic pressure given as a function of a depth and the gravity. The fixed boundary condition is used for the propeller blade control point (at the blade coordinate system origin) and other points at the plane of the control point are kinematically coupled to the control point.

The explicit time integration scheme with the fixed time incrementation is used as a solution method. A variable mass scaling is applied to the Lagrangian propeller blade to obtain a reasonable stable time increment.

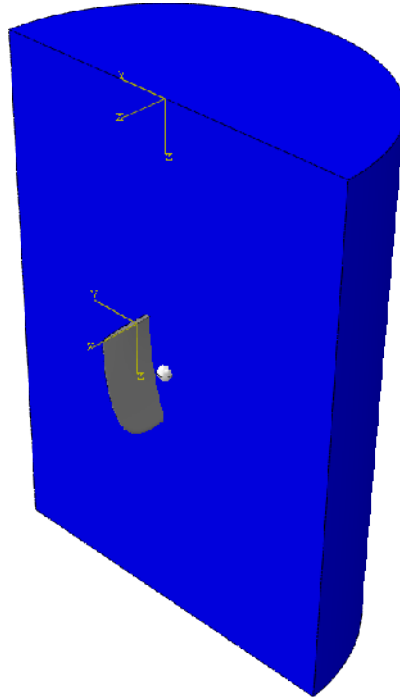


Figure 3. The propeller blade placed to the circular water cylinder. Example of the initial cavity is shown next to the blade.

3. Results

The simulated results with cavitation cloud radius of 0.1 meter were first compared to the earlier field measurements done with the similar size propeller blade (Jussila & Koskinen (1989a, 1989b)) as studied here. The cavitation cloud was in point contact (i.e. $D = 0.0$) with the propeller blade. In Figure 4 is shown the best match of the measured and the simulated blade bending moment results. Note that the sampling frequency of the measured results is only 5 kHz and for the simulated results it is 100 kHz. The presented simulated blade bending moment is observed from the above mentioned propeller blade control point.

The simulated time histories of the forces acting on the propeller blade are presented in Figures 5-8. In each figure cavitation cloud radius is noted with r and D is the smallest distance of the cavitation cloud to the blade. The time of the cavitation void to perfectly collapse is a function of the radius of the spherical void. Therefore the time scale in x-axis varies in Figures 5-8. More importantly, it should be noted that also the force levels vary considerably. The presented maximum forces are integrated variables over the propeller blade.

The maximum impact forces are given as a function of a cavitation cloud maximum radius in Figure 9. It should be emphasized that the maximum impact forces seem to be piecewise linearly dependent from the cavitation cloud radii. The purpose of the Figure 9 is to present a partial starting point for the development of the simplified calculation formulas to be used for the cavitation in general and particularly in ice-induced cavitation. Anyhow, more parameters, such as depth for example, should be taken into account even for simple formulas.

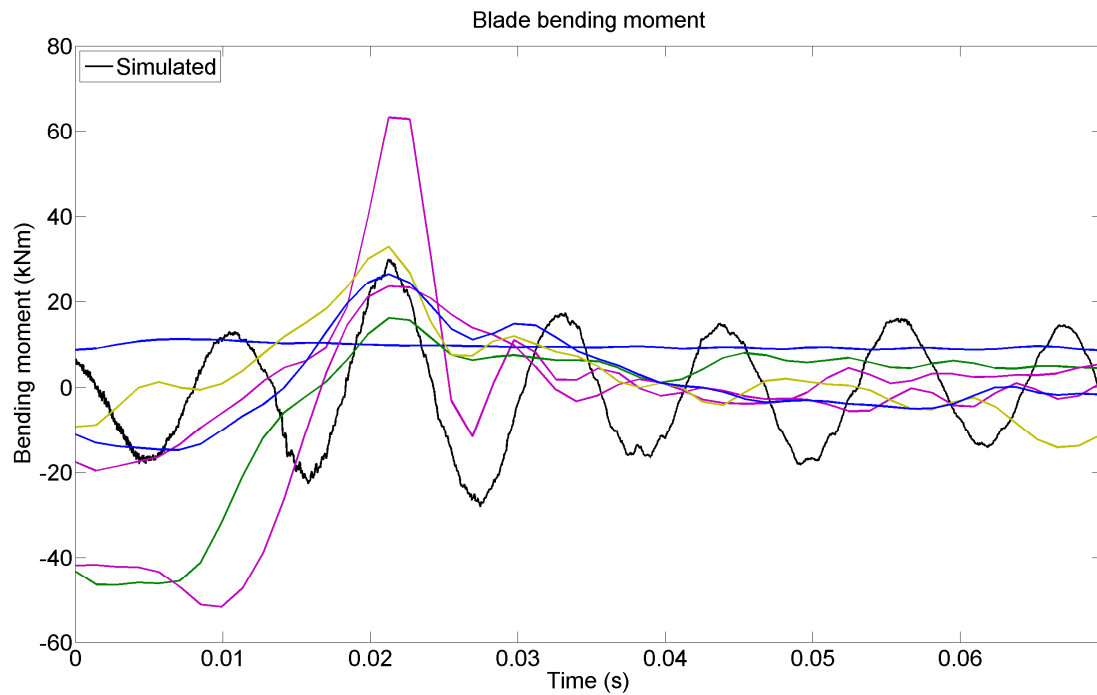


Figure 4. Time histories of the bending moment for the measured and the simulated (black) propeller blade.

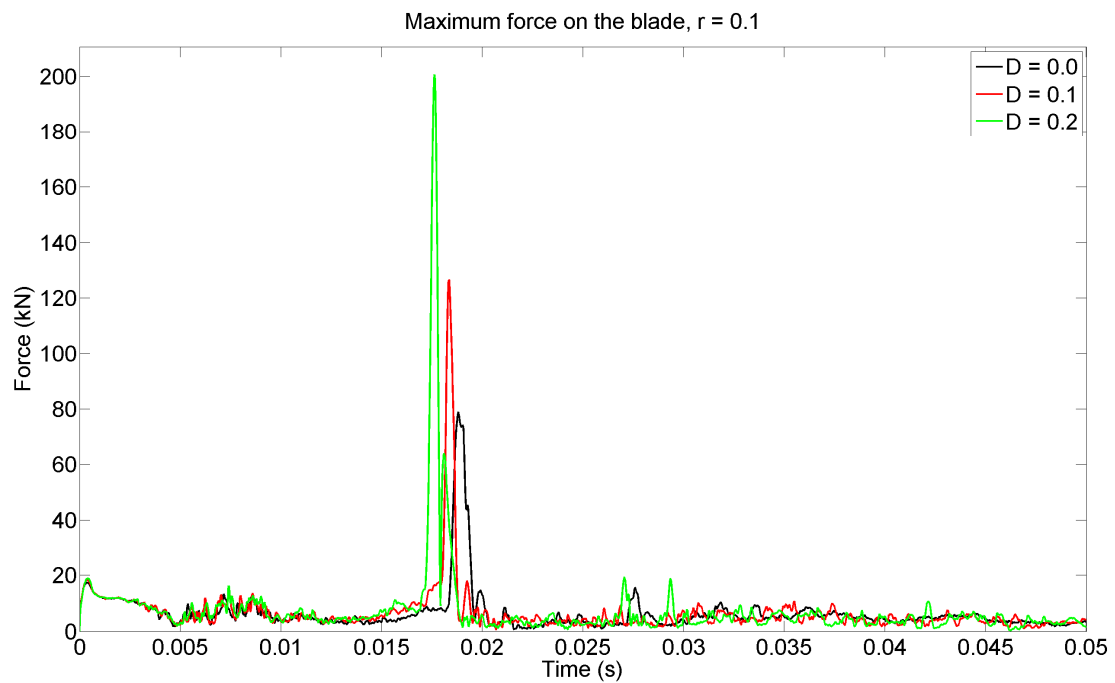


Figure 5. Time histories of the maximum forces on the propeller blade due to cavitation cloud collapse. Cloud radius is 0.1 meters.

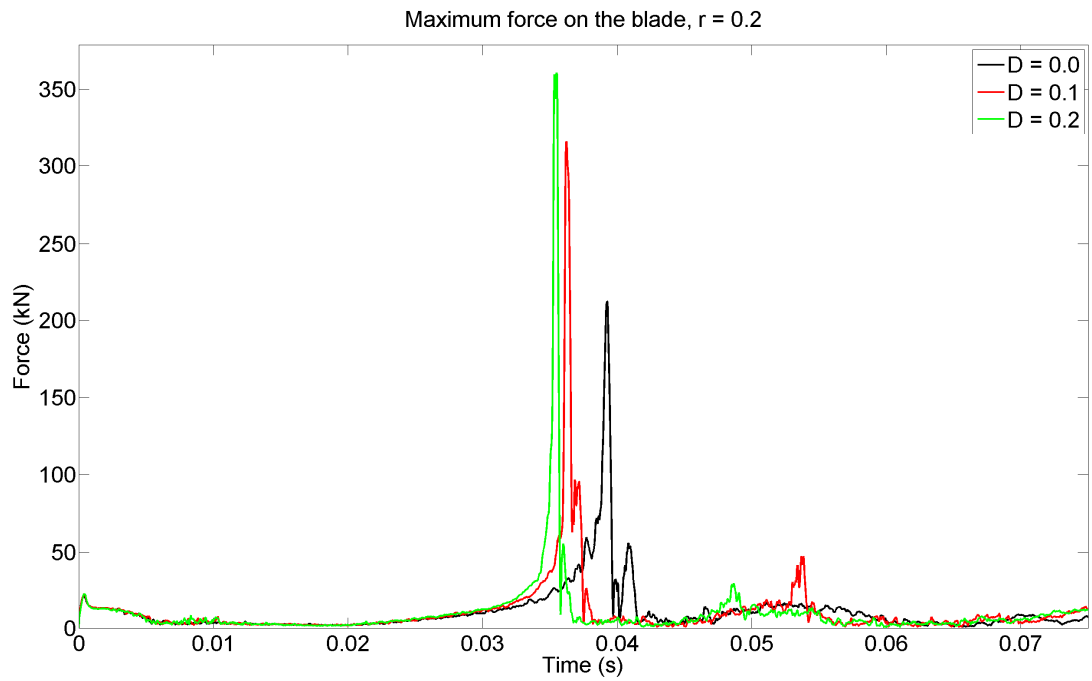


Figure 6. Time histories of the maximum forces on the propeller blade due to cavitation cloud collapse. Cloud radius is 0.2 meters.

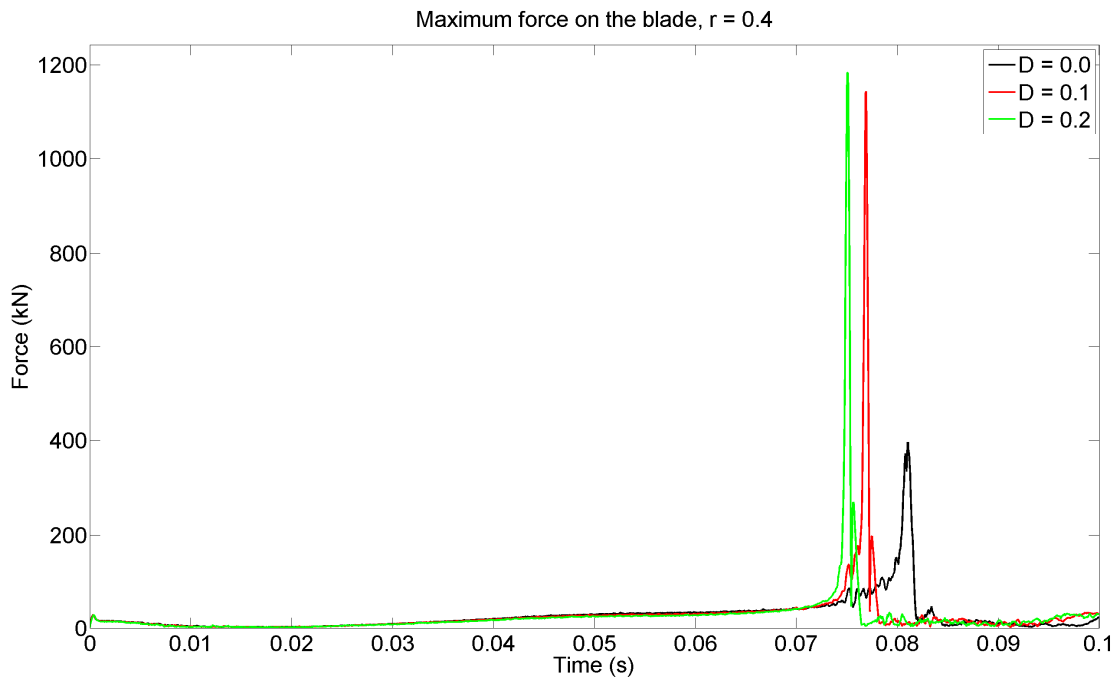


Figure 7. Time histories of the maximum forces on the propeller blade due to cavitation cloud collapse. Cloud radius is 0.4 meters.

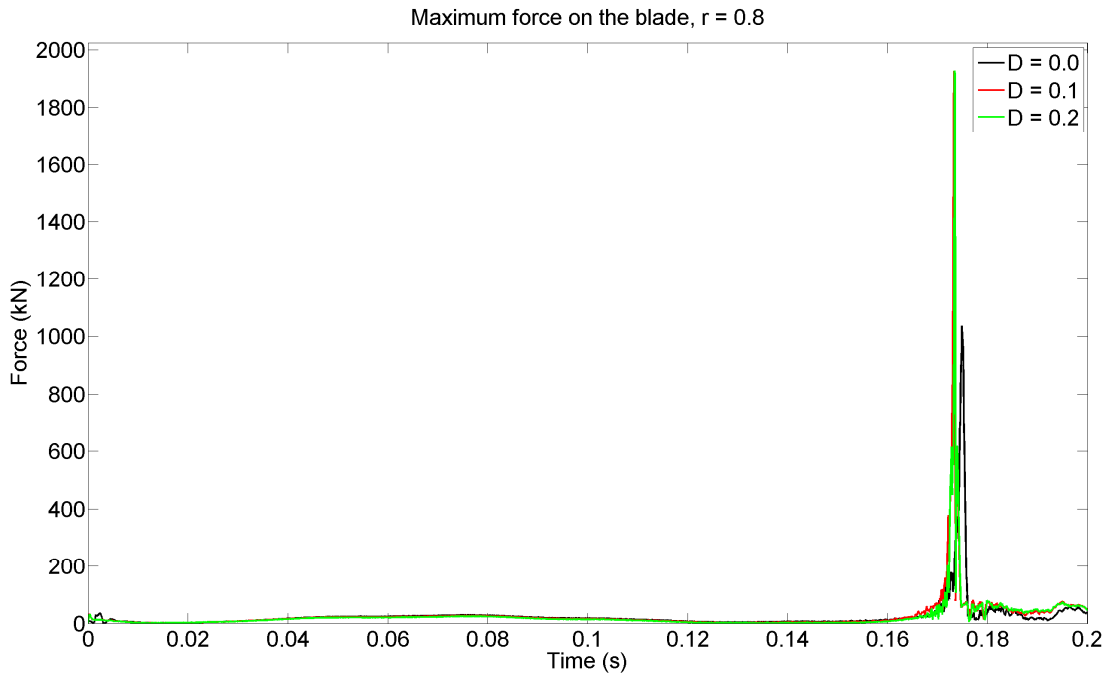


Figure 8. Time histories of the maximum forces on the propeller blade due to cavitation cloud collapse. Cloud radius is 0.8 meters.

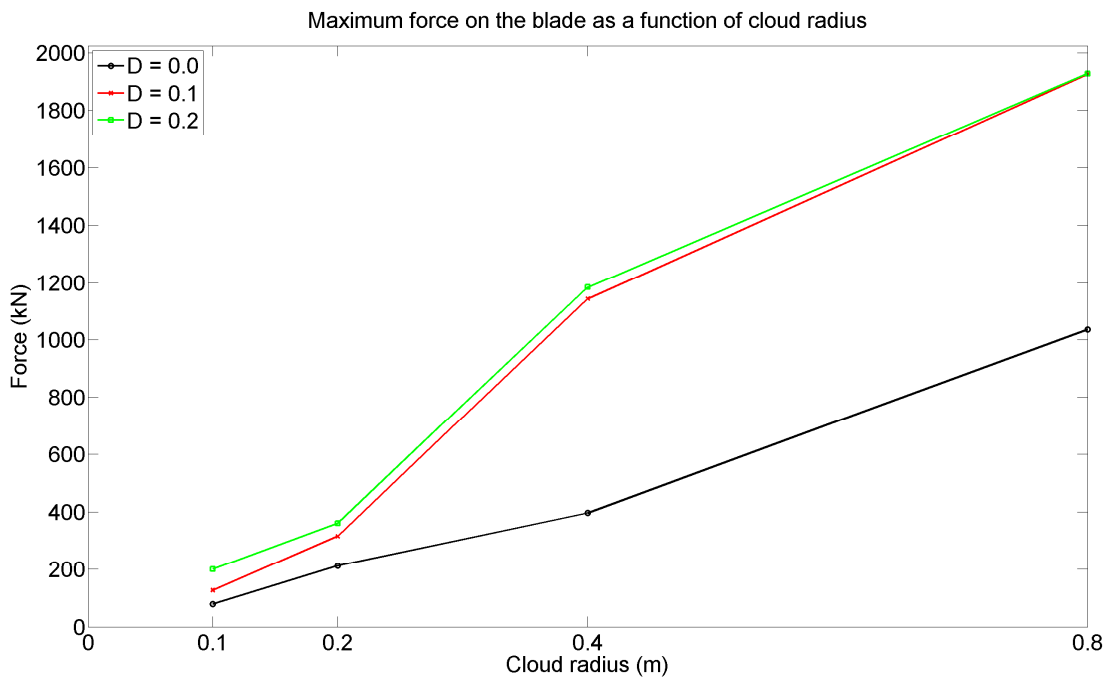


Figure 9. The obtained maximum impact forces as a function of a cavitation cloud maximum radius.

4. Conclusions and discussion

From the results presented in the Figure 4 it can be seen that the trend of the simulated and the measured blade bending moments is quite same. Thus the simulated maximum blade bending moments are in the same order as in the field measurements. The presented results in Figures 5-8 shows that the peak impact forces due to collapse of the ice-induced cavitation clouds are high enough to damage the propeller blade. The presented results do not prevent a possibility that the measured force peaks would be caused by the collapse of the cavitation clouds.

At this point the initial size and shape of the cavitation clouds has been assumed. For further investigations the actual sizes and the variation of the initial cavitation clouds must be known. Therefore the scale model tests are recommended.

References

- Browne, R.P., Keinonen, A., and Semery, P. 1991a. Ice loading on open and ducted propellers. Proceedings of the 1st ISOPE. Edinburgh, Scotland.
- Brown, R.P. and Keinonen, A. 1991b. Icebreaker propulsion systems, propulsive performance and ice loading for design. Proceedings of the 1st Marine Dynamics Conference. St. John's, Canada.
- Duff, J., Kirby, K., and Laskow, V. 1985. Measurement of Ice-Propeller Interaction Parameters: M. V. Robert Lemeur: Main Report. Transport Canada Publication TP 6839E, 271 p.
- ITTC, 2002. ITTC Recommended Procedures and Guidelines, Testing and Extrapolation Methods, Propulsion; Cavitation, Description of Cavitation Appearances. ITTC Report 7.5-02 03-03.2, Revision 1, Propulsion Committee of 23rd ITTC. 7 p.
- Jussila, M. and Koskinen P. 1989a. Ice Loads on CP-Propeller and Propeller Shaft of Small Ferry and Their Statistical Distributions During Winter '87. Proceedings of the 8th International Offshore Mechanics and Arctic Engineering Symposium (OMAE). 19-23 March, 1989, Hague, The Netherlands. Vol. 4, pp. 351-358.
- Jussila, M. and Koskinen P. 1989b. Ice Loads on Propeller Blade of Small Car Ferry. Proceedings of the 10th International Conference on Port and Ocean Engineering under Arctic Conditions (POAC). 12-16 June, 1989, Luleå, Sweden. Vol. 2, pp. 862-872.
- Keinonen, A. and Browne, R. P. 1990. Ice Propeller Interaction Forces. Transport Canada Publication TP 10401E. Vol. 1 & 2, 80 p. + 165 p.
- Laskow, V. & Revill, C. 1986. Engineering analysis of ice/propeller interaction data. Report prepared for the Transportation Development Centre. Calgary, Alberta. Canadian Marine Drilling Ltd. Reports TP 8449E and TP 8450E.
- Lindroos, H. and Björkestam, H. 1986. Hydrodynamic Loads Developed During Ice-Clogging of a Propeller Nozzle and Means to Prevent the Clogging. Proceedings of the International Offshore and Navigation Conference and Exhibition (Polartech '86). 27-30 October, 1986, Helsinki, Finland. Pp. 1061-1092.